

NASA

MEMORANDUM

SUBSONIC AERODYNAMIC CHARACTERISTICS OF SEVERAL
BLUNT, LIFTING, ATMOSPHERIC-ENTRY SHAPES

By Howard F. Savage and Bruce E. Tinling

Ames Research Center
Moffett Field, Calif.

Declassified February 8, 1963

**NATIONAL AERONAUTICS AND
SPACE ADMINISTRATION**

WASHINGTON

January 1959

1G

NATIONAL AERONAUTICS AND SPACE ADMINISTRATION

MEMORANDUM 12-24-58A

SUBSONIC AERODYNAMIC CHARACTERISTICS OF SEVERAL

BLUNT, LIFTING, ATMOSPHERIC-ENTRY SHAPES

By Howard F. Savage and Bruce E. Tinling

SUMMARY

The subsonic aerodynamic characteristics of some possible atmospheric-entry configurations have been determined from wind-tunnel tests. The basic shape was formed by removal of a portion of a blunted 60° cone to form a flat-topped lifting body.

Modifications to this body were investigated which were directed toward obtaining stability and control. These modifications included changes in base shape, rounding of the upper surface edges, addition of a low-aspect-ratio wing, and addition of control surfaces. The results indicate that both winged and wingless blunt vehicles can be made stable at subsonic speeds for moment center locations compatible with hypersonic stability and control requirements.

INTRODUCTION

A vehicle for manned entry into a planetary atmosphere poses severe and somewhat conflicting design requirements in that decelerations must be within human tolerance and, at the same time, the aerodynamic heating must be limited to a value that is safe for both the structure and the occupant. A lifting vehicle with a small lift-drag ratio is attractive for limiting these decelerations and temperatures to tolerable values (see refs. 1 and 2). A further advantage of a lifting vehicle is that the pilot can exercise some measure of control over the landing point once the entry process has been initiated. The vehicle must also be stable and controllable down to a velocity low enough to permit deployment of a parachute or other landing device.

A low lift-drag ratio glider configuration formed by removing essentially the upper half of a high drag body of revolution has been proposed for atmospheric entry of manned satellites. Theoretical estimates of the

motion and heating during entry for a family of half-cone configurations and an experimental investigation of the stability and control characteristics at high supersonic speeds of a particular vehicle indicate that such vehicles may be practical for atmospheric entry (see ref. 2). This report presents the results of subsonic wind-tunnel tests to determine the static stability and control characteristics of a series of lifting configurations. The basic shape was formed by removal of a portion of a blunted 60° cone to form a flat-topped body. The flat-topped body was tested in combination with low-aspect-ratio wings, various base and upper surface fairings, and control surfaces. The tests were conducted in the Ames 12-foot pressure wind tunnel at Mach numbers up to 0.90 at a Reynolds number of 0.5 million, and at Reynolds numbers of 0.6, 2.0, and 3.0 million at a Mach number of 0.25.

NOTATION

The data are presented as force and moment coefficients with lift and drag referred to wind axes and the other force and moment coefficients referred to a body axis system with the longitudinal axis in the plane of symmetry and parallel to the upper surface of the basic body. The moment center was located, with the one exception noted in the discussion, at 71.0 percent of the body length behind the leading edge of the body and 18.1 percent of the body length below the axis of the basic cone. This moment center was selected from hypersonic stability considerations (see ref. 2). The coefficients and symbols used are defined as follows:

b reference span for calculating C_l and C_n ; wing span for winged configurations; and body base diameter for wingless configurations

C_D drag coefficient, $\frac{\text{drag}}{qS}$

C_L lift coefficient, $\frac{\text{lift}}{qS}$

C_l rolling-moment coefficient, $\frac{\text{rolling moment}}{qSb}$

C_m pitching-moment coefficient, $\frac{\text{pitching moment}}{qSl}$

C_n yawing-moment coefficient, $\frac{\text{yawing moment}}{qSb}$

C_Y lateral-force coefficient, $\frac{\text{lateral force}}{qS}$

$$C_{l\beta} \quad \frac{\partial C_l}{\partial \beta}, \text{ per deg}$$

$$C_{n\beta} \quad \frac{\partial C_n}{\partial \beta}, \text{ per deg}$$

$$C_{Y\beta} \quad \frac{\partial C_Y}{\partial \beta}, \text{ per deg}$$

$$\left. \begin{array}{l} \Delta C_l \\ \Delta C_n \\ \Delta C_m \end{array} \right\} \text{ increment in the coefficient due to control deflection, that is,}$$

$$\Delta C_l = C_{l\delta} - C_{l\delta=0}$$

l body length

$\frac{L}{D}$ lift-drag ratio

M free-stream Mach number

q free-stream dynamic pressure

R Reynolds number, based on the body length

S reference area for calculating force and moment coefficients; wing area for winged configurations and body plan-form area for wingless configurations

α angle of attack of the upper surface of the basic body (inclined 6.6° to the cone axis), deg

β angle of sideslip, deg

δ control surface deflection, deg

MODEL

Some of the pertinent geometric details of the models tested are given in figure 1. Photographs of one of the models mounted in the Ames 12-foot pressure wind tunnel are shown in figure 2.

The bodies were portions of a 60° apex angle cone with a nose radius equal to 16.7 percent of the base diameter. As is illustrated in figure 1(a), four of the bodies consisted of the full cone and three flat-topped lifting configurations formed by removing portions of this

cone. The body with the top cut off at an angle of 6.6° to the cone axis and through the apex of the cone was taken as the "basic body" and will be referred to as such. Several other bodies were formed by additions to this basic body. Additions were made to the base of the body which extended the top along the lines of the basic body or extended the bottom either along the basic body line or parallel to the cone center line (fig. 1(a)). The top of the basic body was also changed by the addition of a 0.50-inch thick plate with straight sides tangent to the basic body and sharp top edges, or a 0.50-inch thick plate with a radius of 0.56 inch on the edge (fig. 1(b)).

Wings of two plan forms were used (fig. 1(c)). Two of the wings were $3/16$ inch thick with rounded leading edges. One had a sweepback of 50.0° and a nose radius in plan view 180 percent of the body nose radius. This wing was used only with the basic body and was also tested with the leading edge drooped 30° along the body line, or with the tips drooped 30° about a line parallel to and located one-half base diameter from the plane of symmetry. The sweepback of another wing was 47.6° and the nose radius in plan view was the same as that of the body nose. This wing was used in combination with the basic body or the body with the 0.50-inch rounded top plate (fig. 1(c)), and was also tested with the tips deflected up 30° about a line in the plane of the body base. Another wing with a sweepback of 47.6° had a basic elliptical cross section, as viewed from the rear, with an eccentricity of 0.991 and was filleted to the body (fig. 1(c)). The elliptical wing was also used with the tips cut off at and parallel to the base of the body.

Plain control surfaces were attached to the base of the body at the positions shown in figure 1(b). The top and side controls on the body were all the same size and the bottom control surface had twice the area of the others. The tips of the wing with 47.6° of sweepback for the configuration with the rounded top plate were also used as elevons with hinge lines at and parallel to the body base. The sign conventions used for the various control deflections are shown in figures 1(b) and 1(c).

The model was sting-mounted in the wind tunnel on a 1-inch diameter, six-component strain-gage balance. The balance protruded from the rear of the model and was shielded from the air stream by a 1-1/4-inch-diameter fairing attached to the sting.

TESTS AND DATA REDUCTION

The aerodynamic forces and moments were measured with the six-component strain-gage balance. All configurations were tested at a Mach number of 0.25 and a Reynolds number of 0.6 million over a large range of angles of attack. Selected configurations were also tested at a Mach

number of 0.25 and Reynolds numbers of 2.0 and 3.0 million and at Mach numbers up to 0.90 at a Reynolds number of 0.5 million over a range of angles of attack and sideslip.

No corrections have been applied to the data to account for the induced effects of the tunnel walls resulting from lift on the model or for the effects of constriction due to the tunnel walls. No adjustment was made to the longitudinal force for the base pressure which probably was influenced by the presence of the sting support.

RESULTS AND DISCUSSION

Wingless Configurations

The longitudinal aerodynamic characteristics of several body shapes are presented in figure 3. As the top of the cone was cut back successively to 1.90 and 1.20 inches above the cone axis, the lift coefficient and lift-drag ratio increased. For example, at an angle of attack of 0° of the cone axis ($\alpha = -6.6^\circ$ for the reference axis system chosen for this report), removing the top of the cone to within 1.20 inches of the cone axis increased the lift coefficient from 0 to about 0.6 and changed the lift-drag ratio from 0 to about 0.7. When the cone was cut along a plane passing through the cone apex and inclined 6.6° to the cone axis (which represents what will be called the "basic body"), a maximum lift coefficient of about 0.95 was obtained at a lift-drag ratio of about 0.88. The choice of an inclination of 6.6° is purely arbitrary and was not dictated by aerodynamic considerations. It should be noted that the pitching-moment coefficients presented in figure 3 are arbitrarily referred to a moment center located on the cone axis. The moment center for the data of subsequent figures is 18.1 percent of the body length below the cone axis. This moment center was chosen on the basis of hypersonic stability and control considerations (see ref. 2). Comparison of the pitching-moment coefficients of the basic body with the two moment center locations (figs. 3 and 4) indicates that the main effect of lowering the moment center was to increase the out-of-trim pitching moment while the instability at small angles of attack remained about the same.

The variation of pitching-moment coefficient with angle of attack for the basic body with the lower moment center indicates longitudinal instability up to maximum lift and the necessity for a relatively large balancing moment for trim. In an attempt to alter these characteristics, several modifications of the base were tested and the results are presented in figure 4. It is noted that some of the modifications had powerful effects on the pitching moments. With a proper choice of base shape and a small change in the location of the center of gravity, the

body with the bottom extended along the basic body line could be trimmed and would have longitudinal stability throughout the angle-of-attack range of interest.

The body shapes for the data presented in figures 3 and 4 had sharp edges where the upper portion of the cone was removed. Such an edge could not be tolerated under the conditions of aerodynamic heating encountered during atmospheric entry. In order to ascertain the effect of rounding the edges, a half-inch plate with the plan form of the body was added to the top of the basic body, and tests were made with a sharp upper edge and with a 0.56-inch radius on the upper edge. As might be expected (see fig. 5), the addition of the plate with the sharp edge had only a small and about constant effect on the lift, drag, and pitching-moment coefficients over the angle-of-attack range investigated. Rounding the upper edge reduced the lift and drag at a given angle of attack and eliminated the sudden changes in forces and moments that occurred near maximum lift. For example, rounding the upper edge reduced the lift coefficient at an angle of attack of 0° from about 0.67 to 0.58 and L/D remained unchanged at about 0.75. In addition, rounding the upper edge provided a large increase in longitudinal stability up to near maximum lift.

Winged Configurations

Several benefits may be expected to accrue from combining a wing with the body at the expense of complicating the aerodynamic heating problem. Among these is a greater control over the lift-drag ratio and, hence, over the trajectory and choice of landing location. The trailing portions of a wing also would provide a convenient location for control surfaces. Therefore, several winged configurations were tested and the results are presented in figure 6. The model with the wing having the flat upper surface with 50° of sweepback (nose radius in plan view 180 percent of body nose radius) had large static longitudinal stability changes throughout the angle-of-attack range of interest. Reducing the sweepback to 47.6° (nose radius in plan view equal to that of the body nose) and combining this change with the body extending upward through the wing provided improvements in longitudinal stability.

Several other modifications to the wings were tested and the results are presented in figure 7. The effects of deflecting the wing leading edge and wing tips are shown in figure 7(a) and compared with the characteristics of the wing with 50° of sweepback in combination with the basic body. Drooping the leading edge 30° along a line coincident with the body line reduced the longitudinal instability of the model but also reduced the lift-drag ratio from about 1.4 to about 1.1 at zero angle of attack; while drooping the wing tips 30° along a line parallel to the body axis produced only small changes in stability and lift-drag ratio. The tips of the 47.6° sweptback wing, in combination with the body with

the rounded top, were deflected up 30° about a line in the plane of the model base. A large increase in static stability was obtained along with a nearly linear variation of pitching moment with angle of attack. This might indicate that the nonlinear pitching-moment variations and the instability of the winged configurations arise from flow separation near the tips of the wings. Deflecting the tips up, of course, increased the out-of-trim pitching moments and decreased the lift coefficient by about 0.3.

Improved pitching-moment characteristics and greater maximum lift (compared to the 50° sweptback wing and basic body combination) were obtained by increasing the leading-edge radius and making the wing cross section elliptical (see figs. 1(c) and 7(b)). A wing with a larger leading-edge radius would also present a less severe heating problem at the leading edge at hypersonic speeds.

Effects of Reynolds Number

The effects of Reynolds number were studied for two of the wingless configurations and two of the winged configurations in the range of Reynolds numbers from 0.6 to 3.0 million at a Mach number of 0.25. The data obtained with the body with the sharp edge (fig. 8) show no significant effect of Reynolds number indicating that the flow separations probably initiated very near the leading edge at all test Reynolds numbers. On the other hand, the data for the body with the rounded edges (fig. 9) show a significant decrease in drag and pitching-moment coefficients as the Reynolds number was increased from 0.6 to 2.0 million and no change as the Reynolds number was further increased to 3.0 million.

The effects of Reynolds number on two of the winged configurations are shown in figures 10 and 11. In each case, increasing the Reynolds number decreased the drag coefficient and the out-of-trim pitching-moment coefficient. For the 47.6° sweptback wing in combination with the basic body (fig. 10), increasing the Reynolds number increased the angle of attack at which a large loss in lift and change in pitching moment occurred. When a rounded top plate was added to the upper surface (see fig. 1(c)) this change in critical angle of attack with Reynolds number did not occur, as is illustrated in figure 11.

Effects of Roughness

In an attempt to simulate the effects of possible erosion of the vehicle during its descent, the models were tested with roughness in the form of number 60 grit sparsely applied to the body nose and over the leading edge of the elliptical wing or over the rounded edge of the body

with the rounded top plate. The results are presented in figure 12. The roughness had only a small effect on the longitudinal characteristics of the body with the rounded edges but had a rather large effect on the lift and pitching moment of the elliptical wing configuration at angles of attack greater than about 4° .

Effects of Mach Number

The body with the rounded top plate, the 47.6° sweptback wing in combination with the basic body, and the 47.6° sweptback wing in combination with the body with the rounded top plate were tested at Mach numbers up to 0.90 and the results are presented in figures 13, 14, and 15, respectively. The drag coefficients of the three configurations increased with increasing Mach number as would be expected, and there were only small changes in the rate of change of pitching moment with angle of attack at the low angles of attack. As the Mach number was increased the maximum lift was reached at progressively lower angles of attack for all three configurations. However, the variations of lift and pitching moment with Mach number were smaller for the wingless configuration (fig. 13).

Lateral and Directional Characteristics

The angle of sideslip was varied at an angle of attack of about 10.5° in order to determine the lateral and directional stability characteristics of the 50° sweptback wing in combination with the basic body, the body with the rounded top plate, and the elliptical wing configuration with the wing tips removed. The results are presented in figure 16 for a Mach number of 0.25 and in figure 17 for a range of Mach numbers. The configurations tested had positive effective dihedral and static directional stability throughout the sideslip and Mach number range investigated. The body with the rounded top edge had more directional stability and more effective dihedral than the winged configuration (fig. 17).

Control Effectiveness

The controls investigated are shown in figures 1(b) and 1(c). For most of the runs only one control at a time was attached to the left side of the model and deflected. For the runs with both the left and right controls attached (wing tip controls and lower side controls), the left control was deflected. The results are presented in figure 18 for angles of attack of 0° and 12° . To check the possibility of interference

effects, one run was made with both lower side controls attached to the model. The indicated interference effects, not presented, were small and of the order of magnitude of the experimental scatter in the data.

The wing tip controls provide pitch and rolling control and the yawing moment remains small. The wingless configuration, on the other hand, requires the top controls for roll control and at least the lower side controls for yaw and pitch control. Different amounts of pitch-yaw interaction could be obtained by changing the control locations on the circumference of the body base.

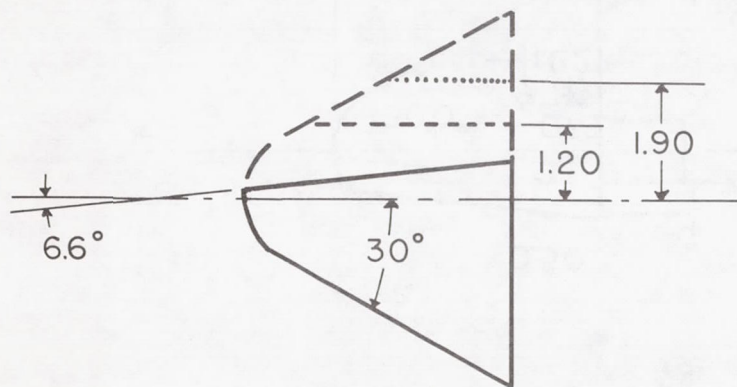
CONCLUDING REMARKS

The aerodynamics of blunt, lifting vehicles of the type required to satisfy heating and deceleration requirements of controlled atmospheric entry is a relatively new and unexplored field. The results of this exploratory wind-tunnel investigation serve to indicate some of the subsonic aerodynamic characteristics of several such configurations capable of operating at lift-drag ratios of the order of 1. It is indicated that there are both wingless and winged configurations which could be made stable at subsonic speeds.

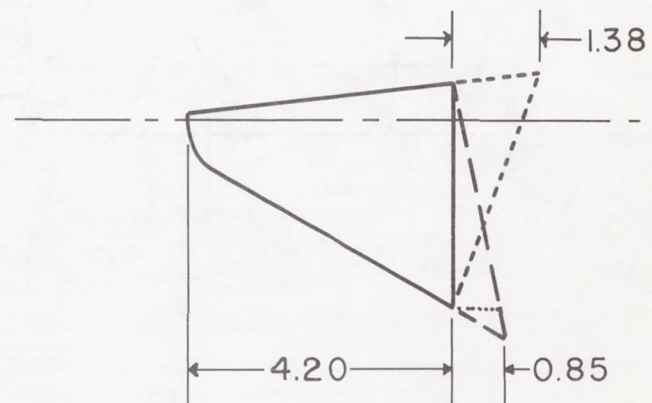
Ames Research Center
National Aeronautics and Space Administration
Moffett Field, Calif., Sept. 24, 1958

REFERENCES

1. Chapman, Dean R.: An Approximate Analytical Method for Studying Entry Into Planetary Atmospheres. NACA TN 4276, 1958.
2. Eggers, Alfred J., Jr., and Wong, Thomas J.: Re-entry and Recovery of Near-Earth Satellites, With Particular Attention to a Manned Vehicle. NASA MEMO 10-2-58A, 1958.



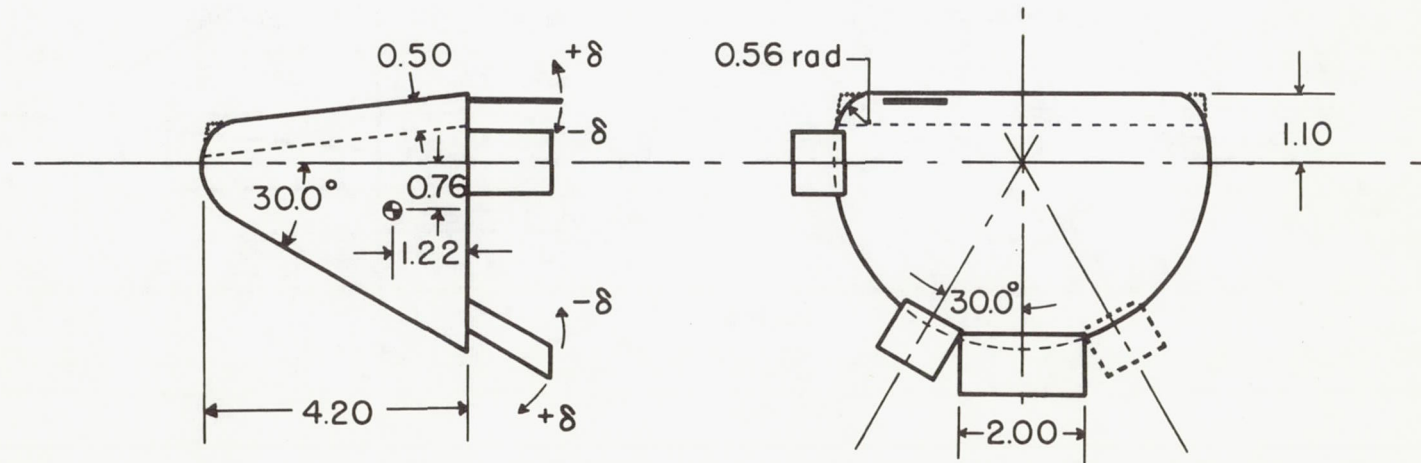
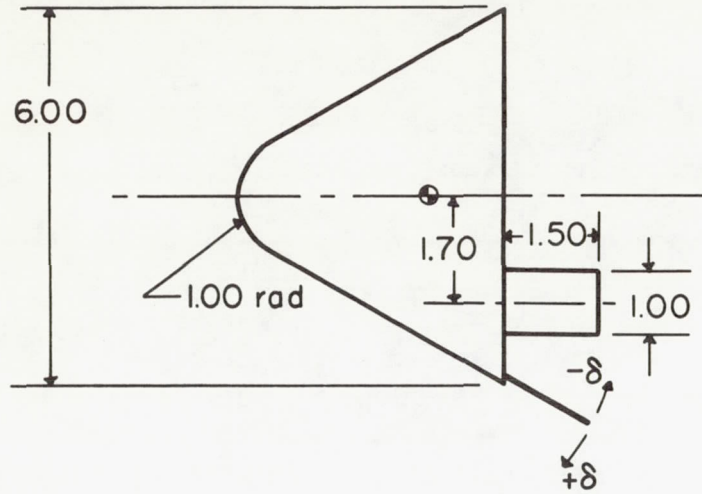
Top modifications



Base modifications

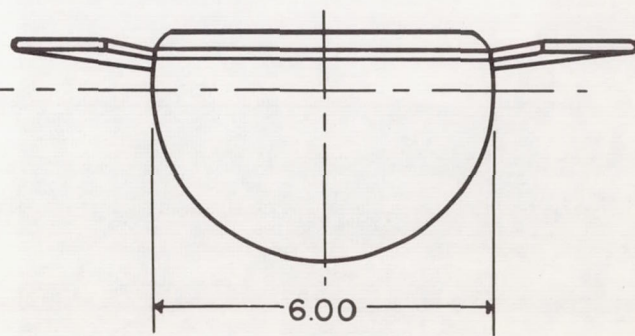
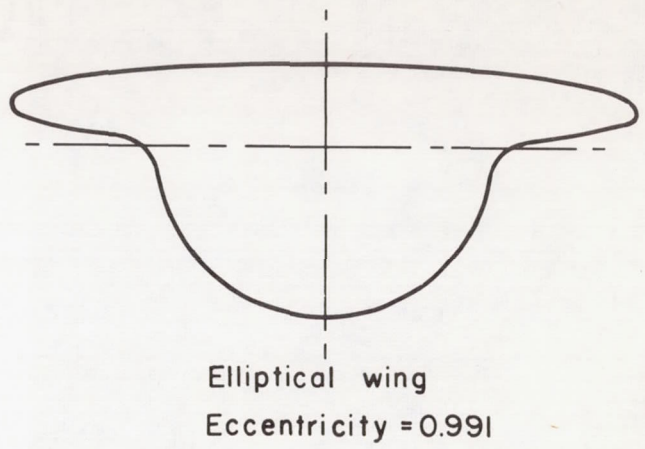
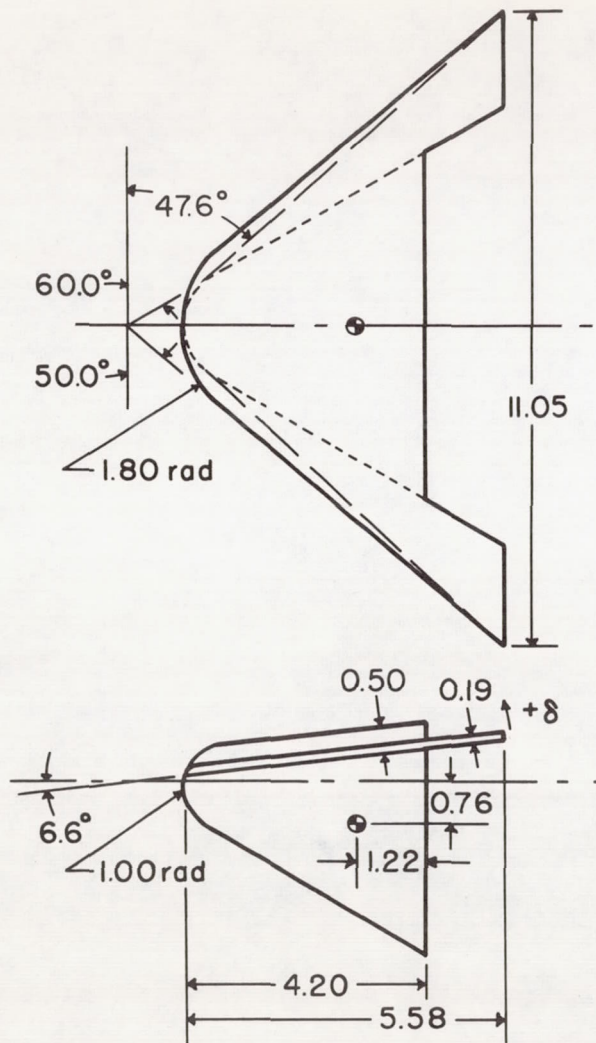
(a) Body modifications.

Figure 1.- Geometry of the model; all dimensions in inches.



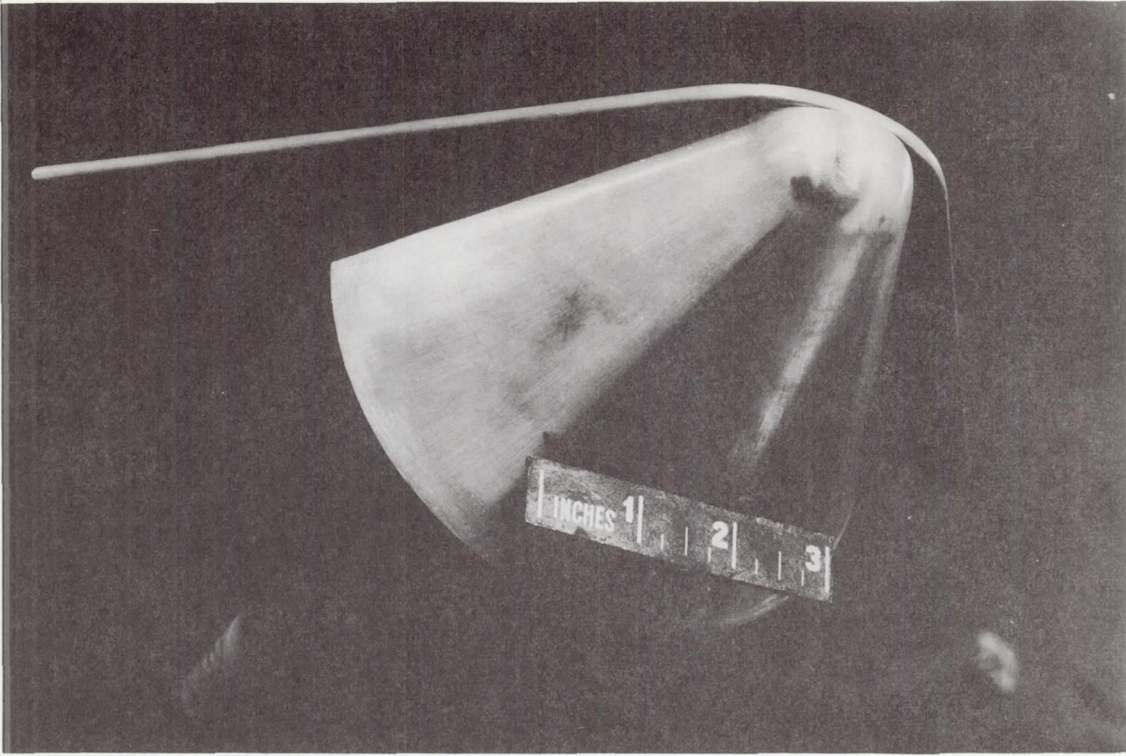
(b) Body controls.

Figure 1.- Continued.

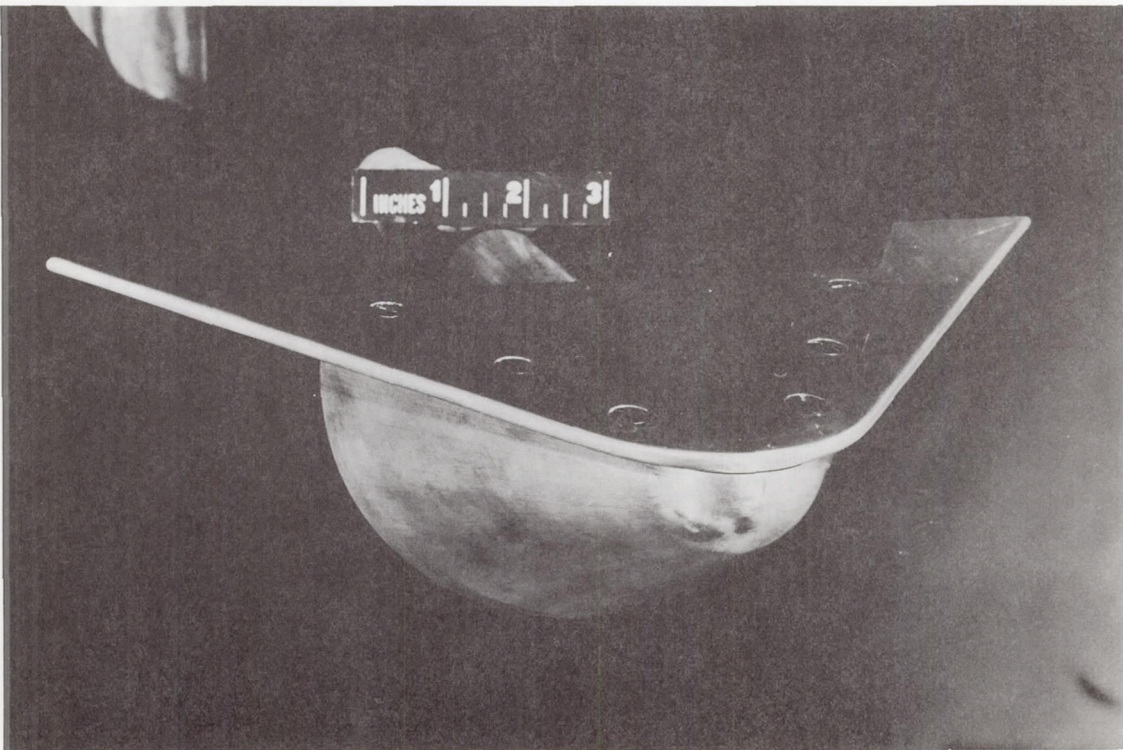


(c) Wings and bodies.

Figure 1.- Concluded.



A-23382



A-23383

Figure 2.- Photographs of the model in the wind tunnel.

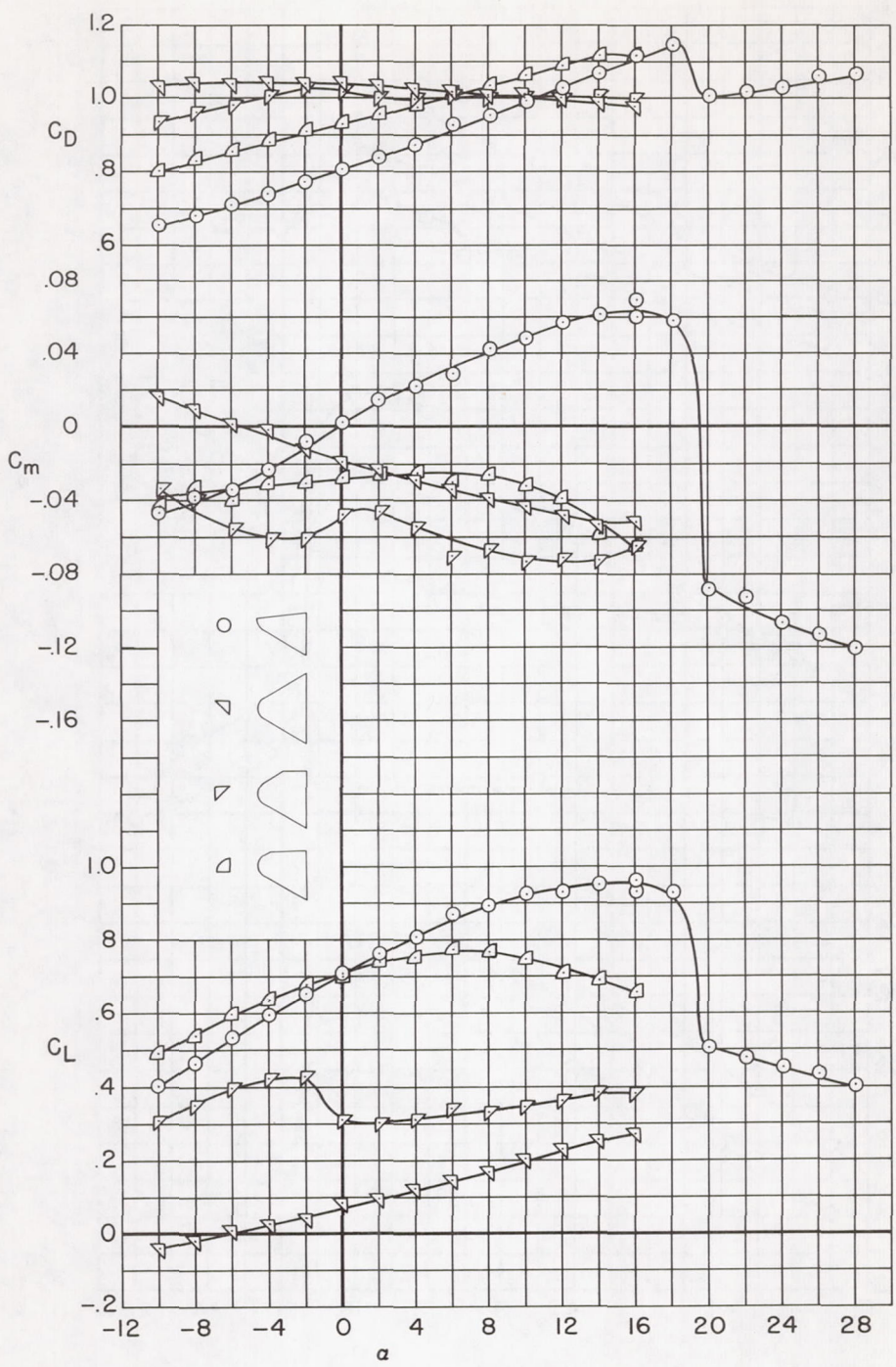


Figure 3.- The longitudinal aerodynamic characteristics of several bodies formed by removing portions of the upper half of a 60° apex angle, blunted cone; moment center on cone axis; M = 0.25, R = 0.6 million.

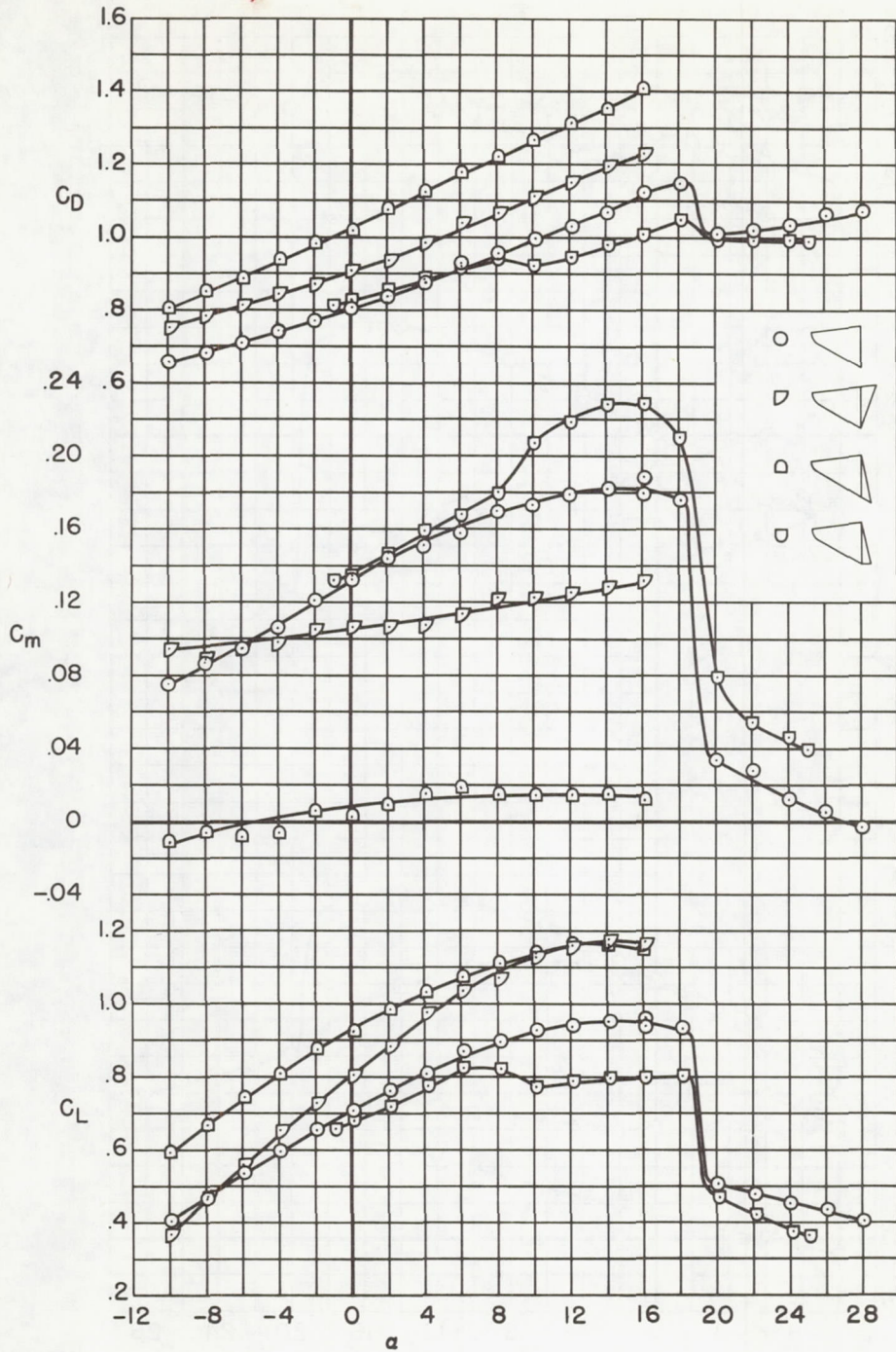


Figure 4.- The effects of changes in base shape on the longitudinal aerodynamic characteristics; $M = 0.25$, $R = 0.6$ million.

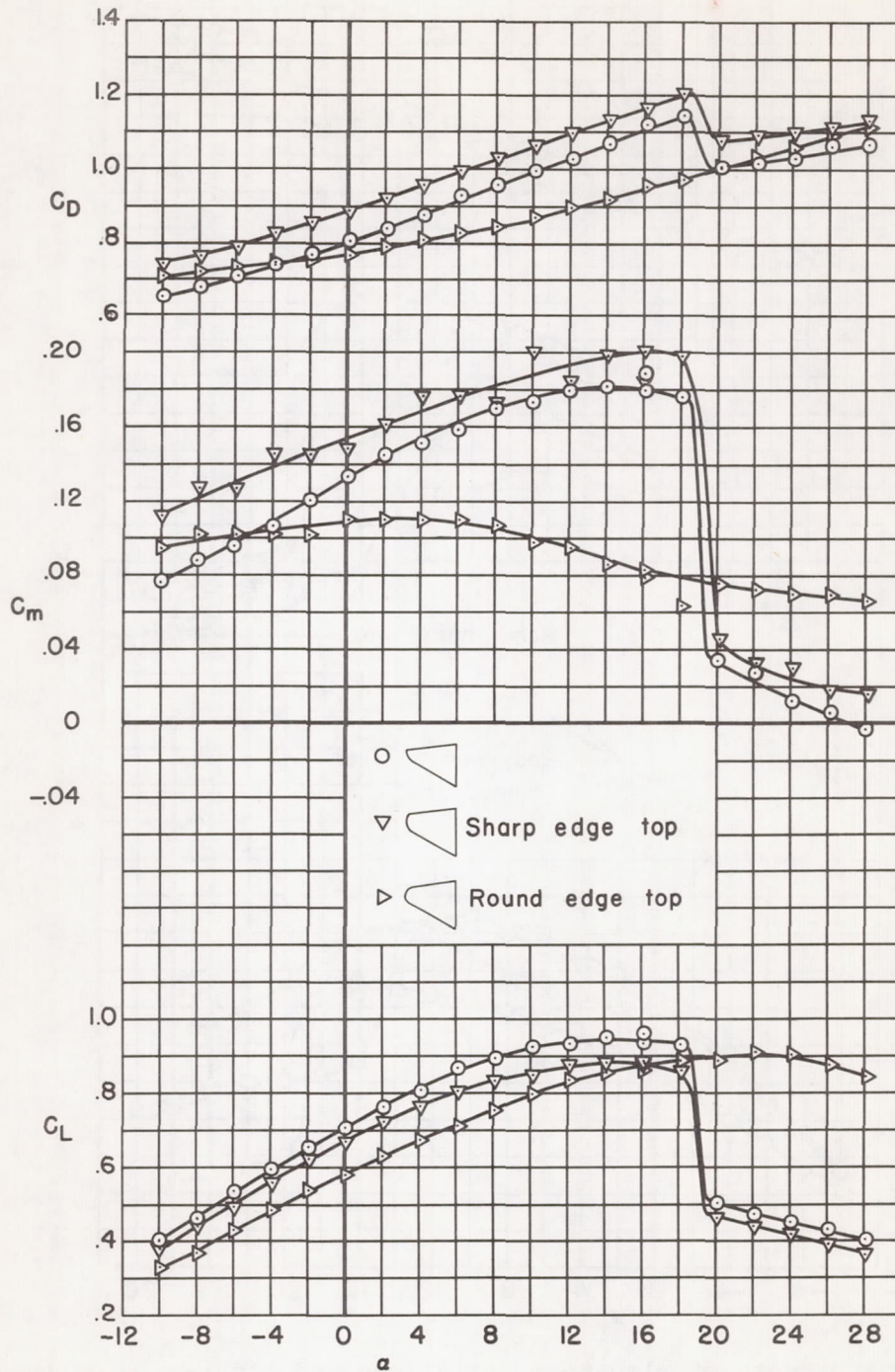


Figure 5.- The effects of rounding the top edge of the body on the longitudinal aerodynamic characteristics; $M = 0.25$, $R = 0.6$ million.

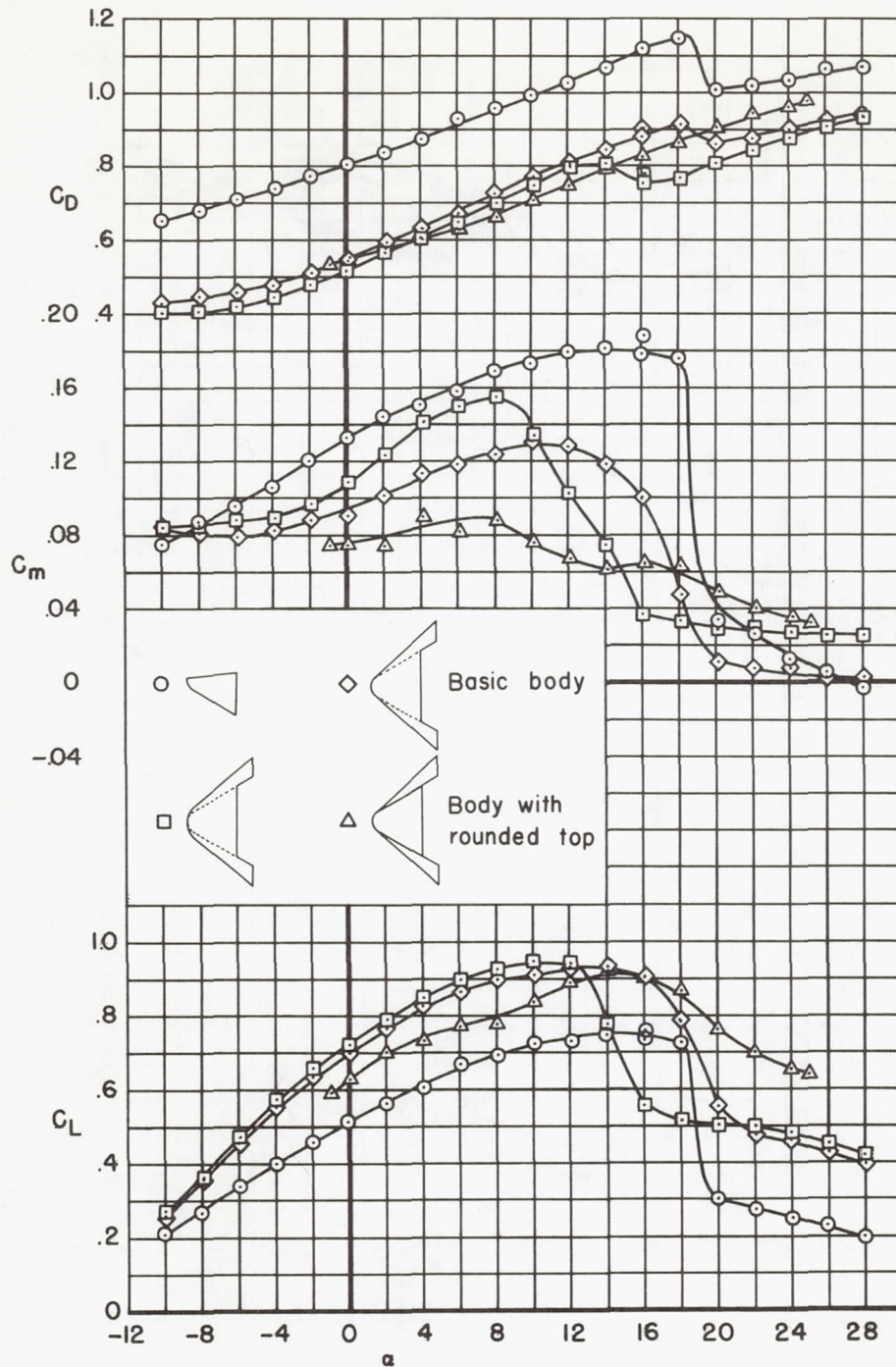
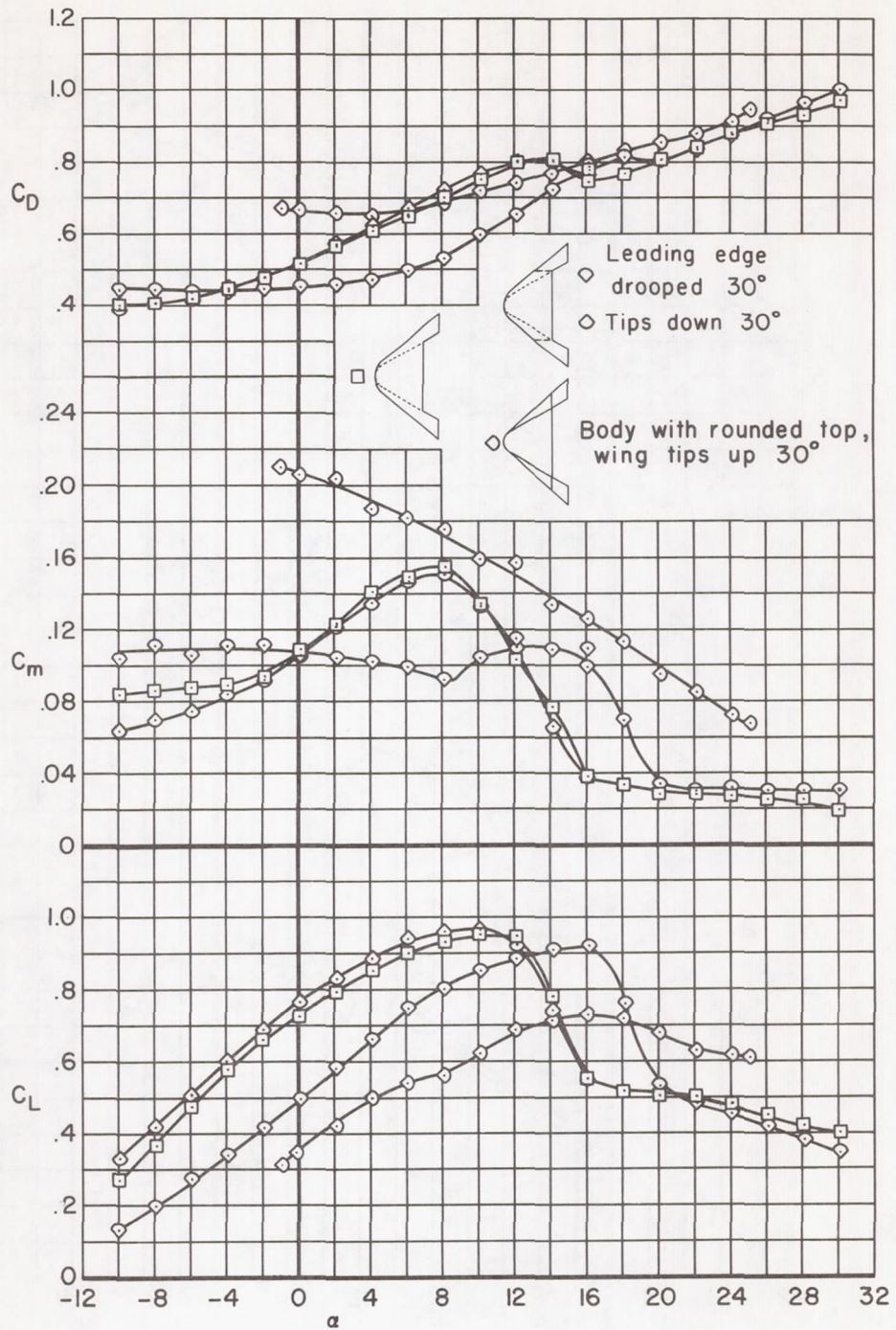
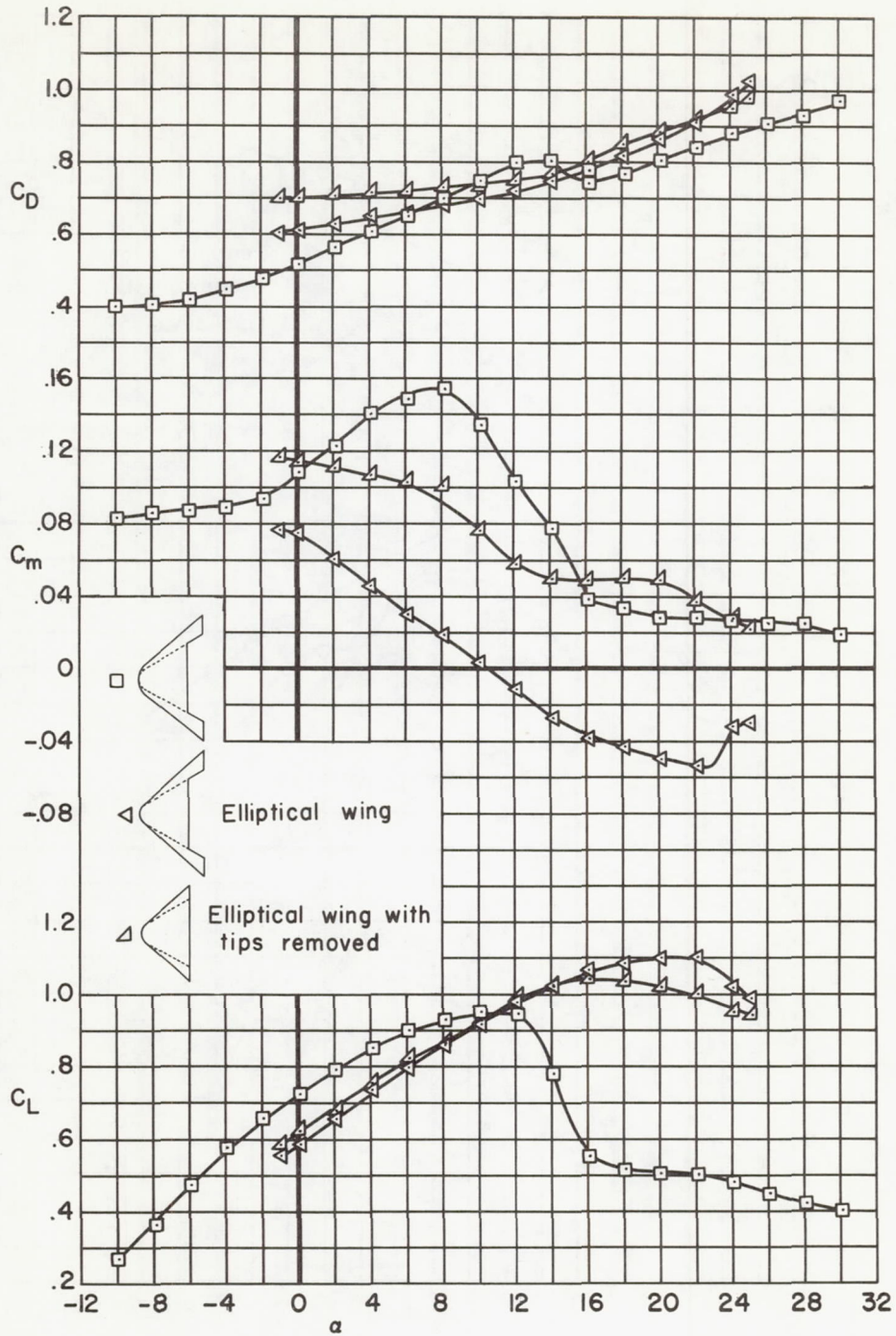


Figure 6.- The effects of plan-form variations and body shape on the longitudinal aerodynamic characteristics of some winged configurations; $M = 0.25$, $R = 0.6$ million.



(a) Effects of wing tip and leading-edge deflections.

Figure 7.- The effects of wing modifications on the longitudinal aerodynamic characteristics; $M = 0.25$, $R = 0.6$ million.



(b) Effects of wing plan form and cross section.

Figure 7.- Concluded.

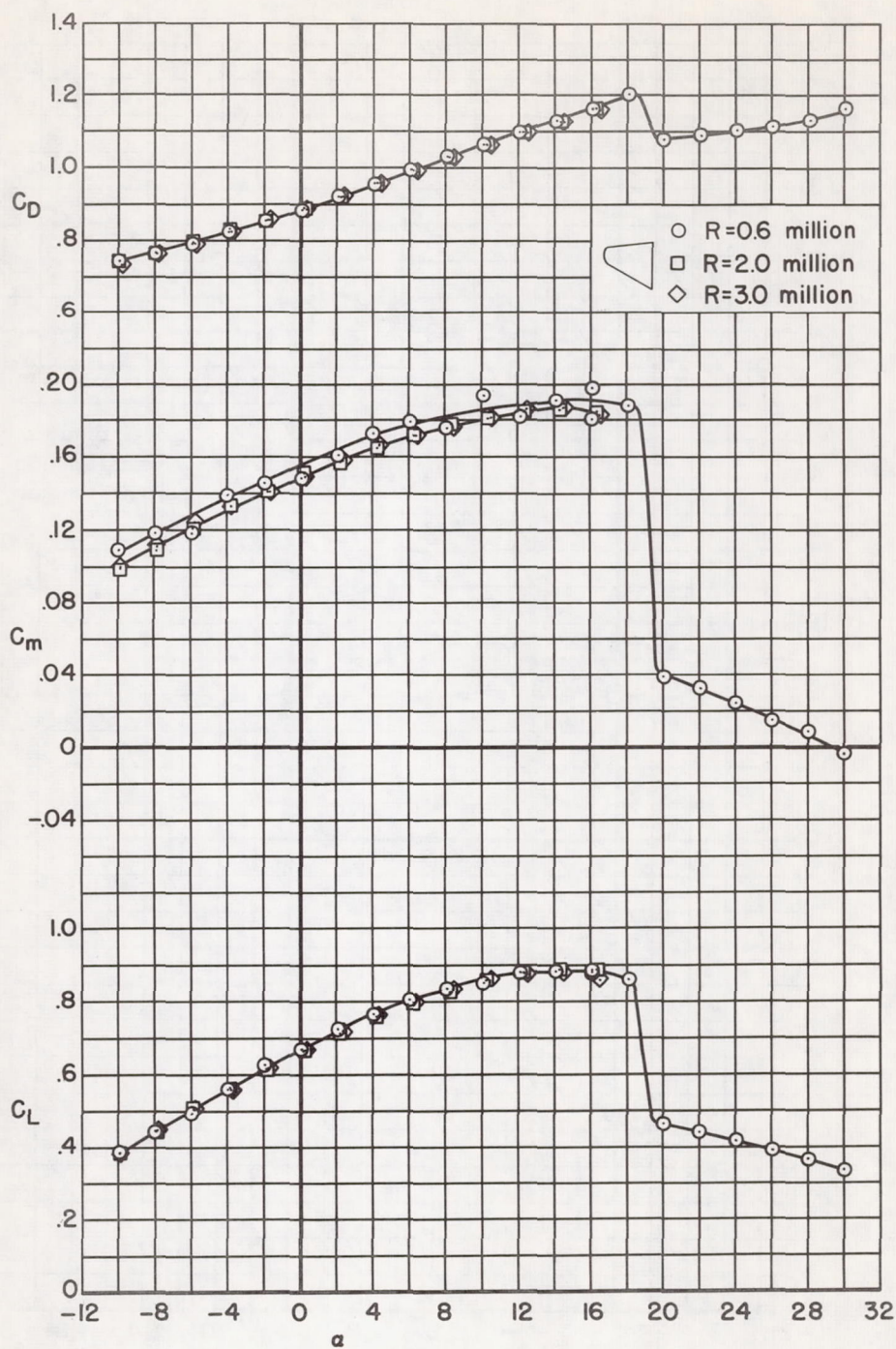


Figure 8.- The effects of Reynolds number on the longitudinal aerodynamic characteristics of the body with the sharp top edge; $M = 0.25$.

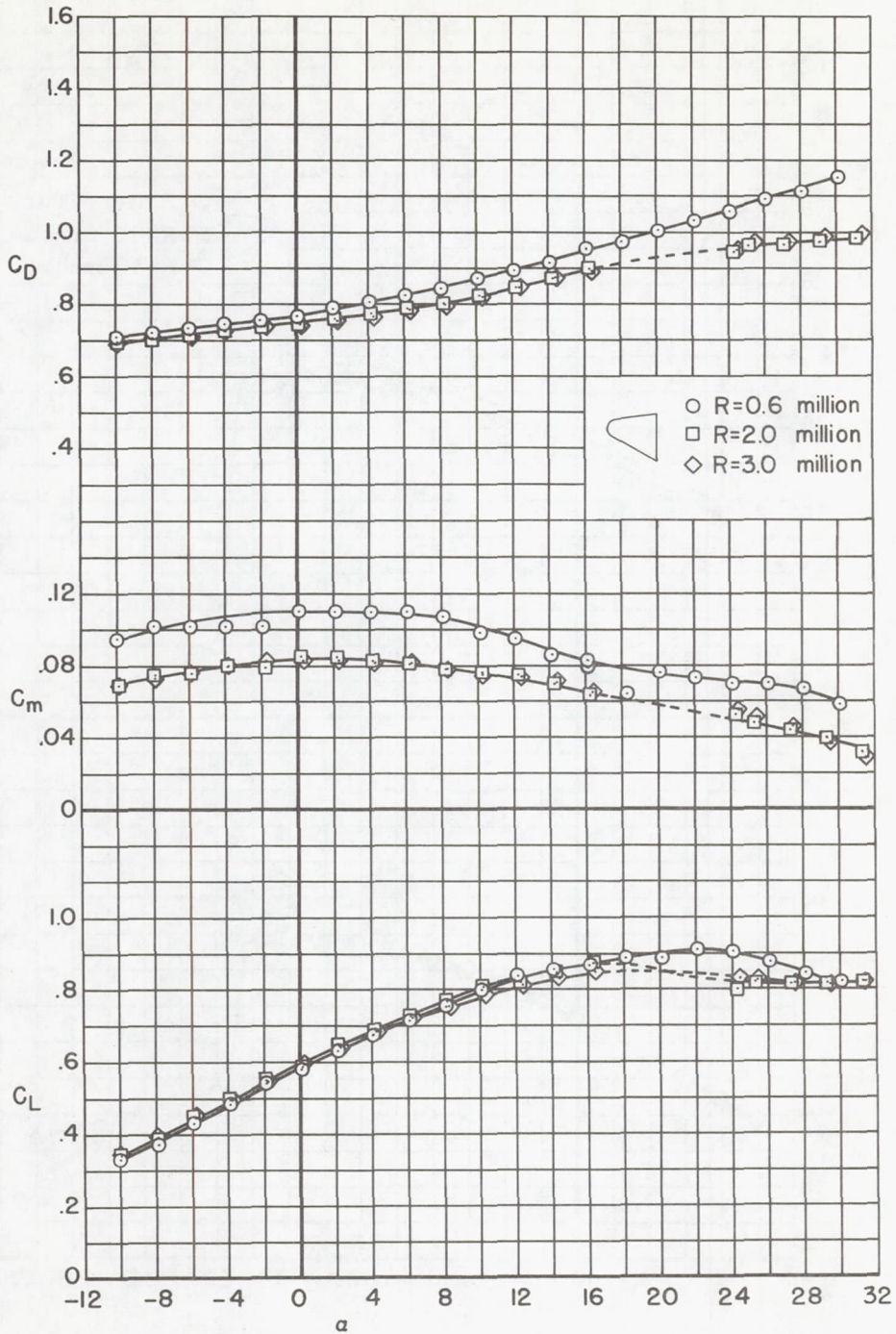


Figure 9.- The effects of Reynolds number on the longitudinal aerodynamic characteristics of the body with the rounded top edge; $M = 0.25$.

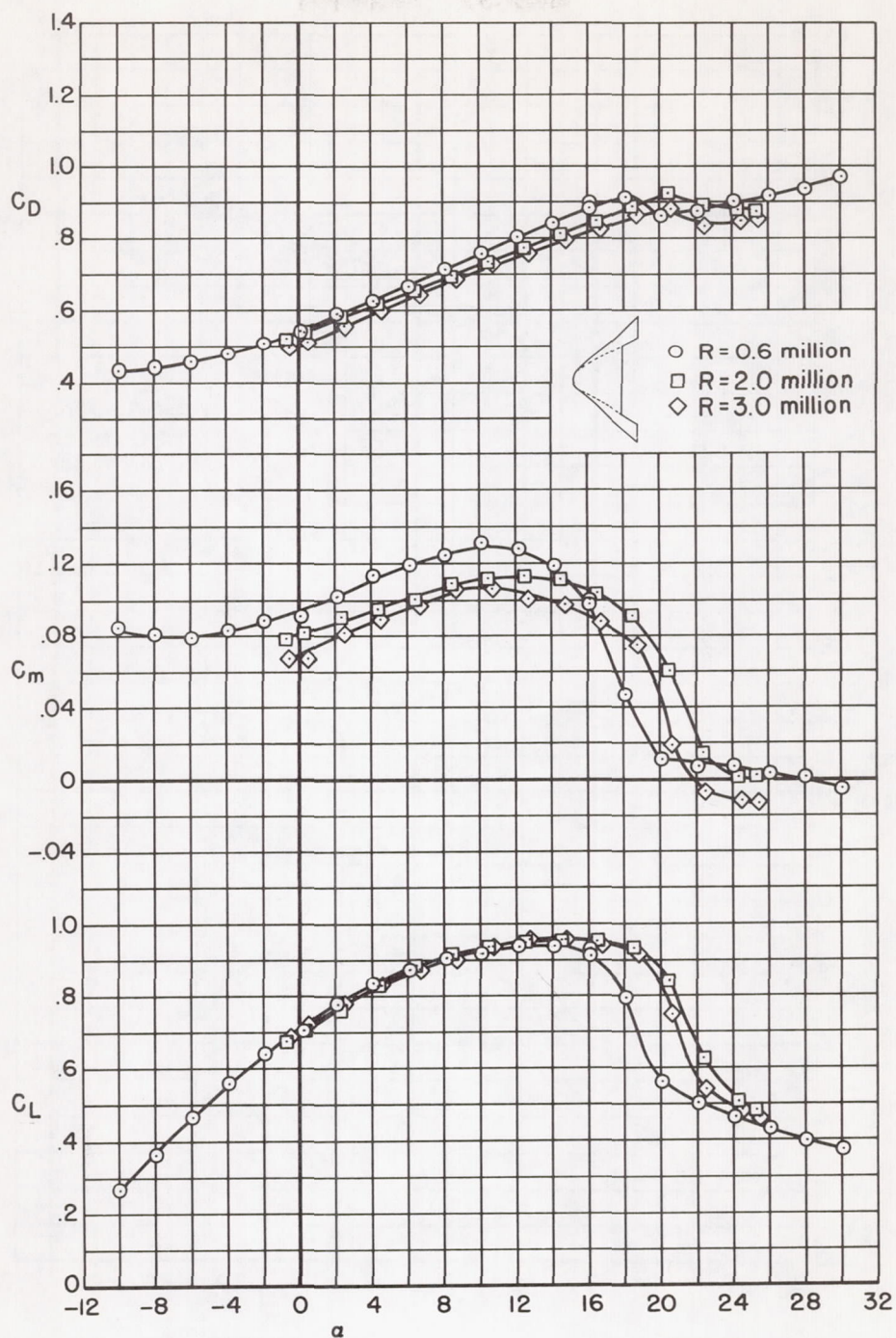


Figure 10.- The effects of Reynolds number on the longitudinal aerodynamic characteristics of the model with the basic body and the 47.6° sweptback wing; $M = 0.25$.

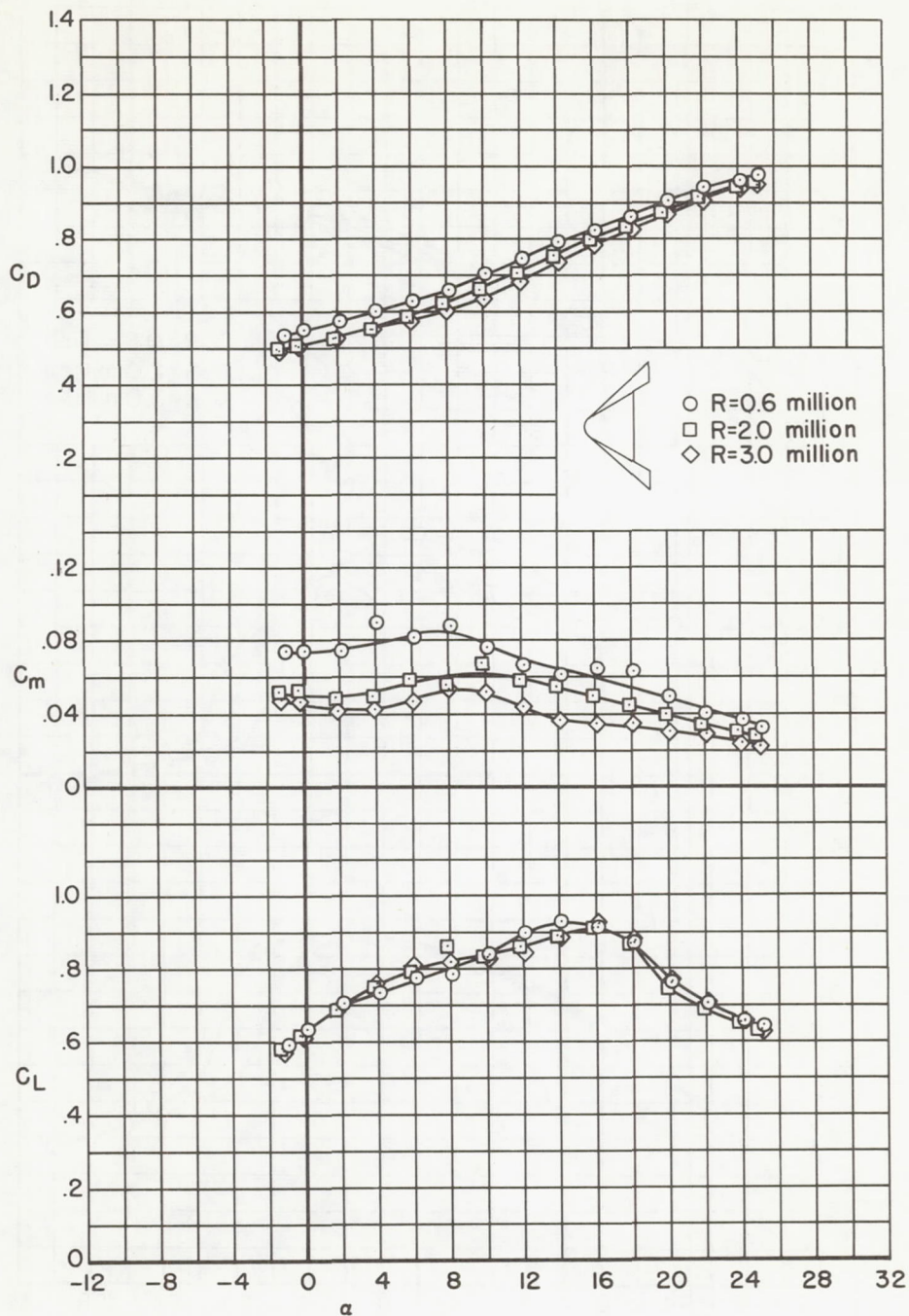


Figure 11.- The effects of Reynolds number on the longitudinal aerodynamic characteristics of the model with the body having the rounded top edge and the 47.6° sweptback wing; $M = 0.25$.

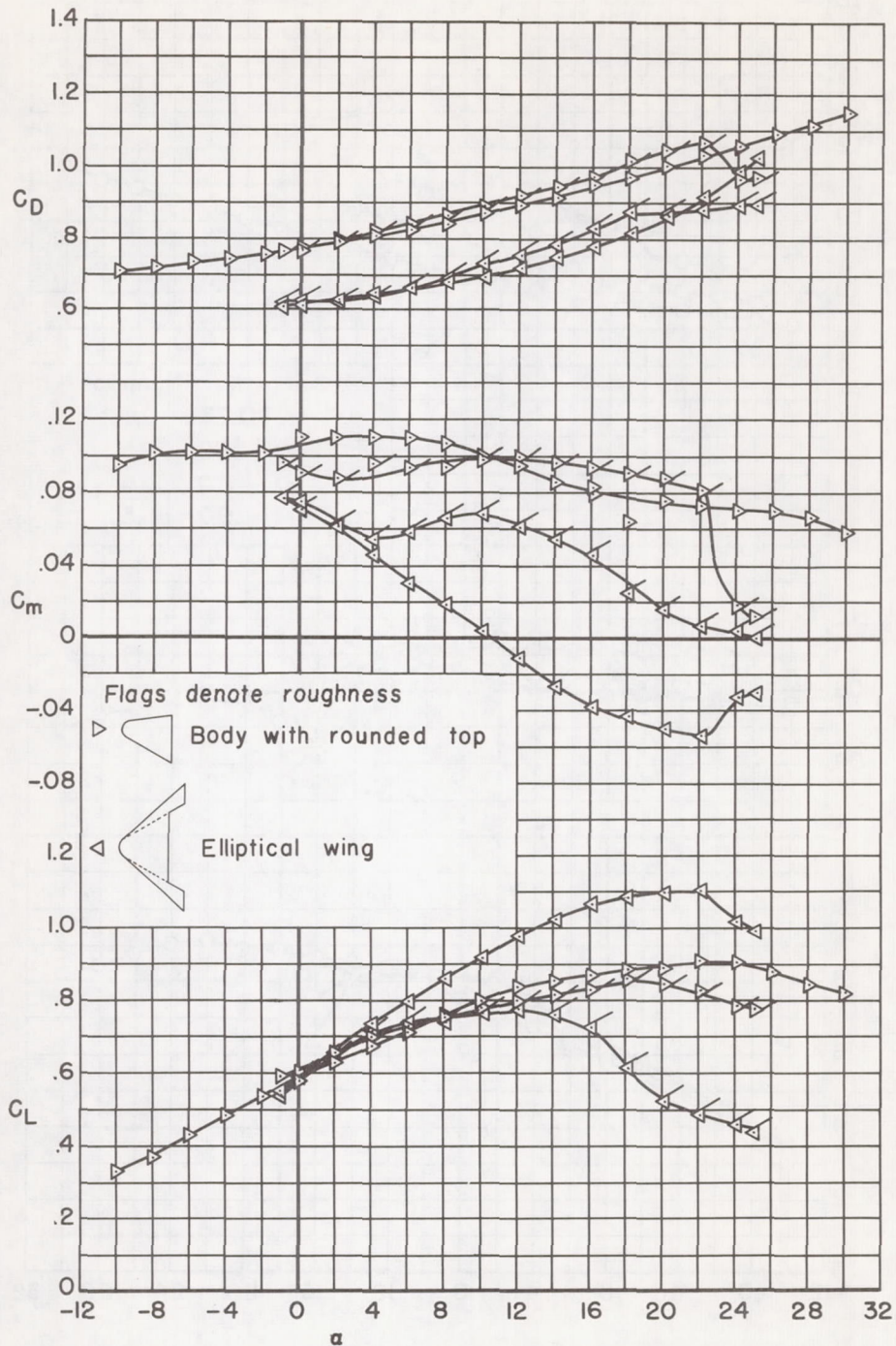


Figure 12.- The effects of roughness on the longitudinal aerodynamic characteristics of a wingless and an elliptical wing configuration; $M = 0.25$, $R = 0.6$ million.

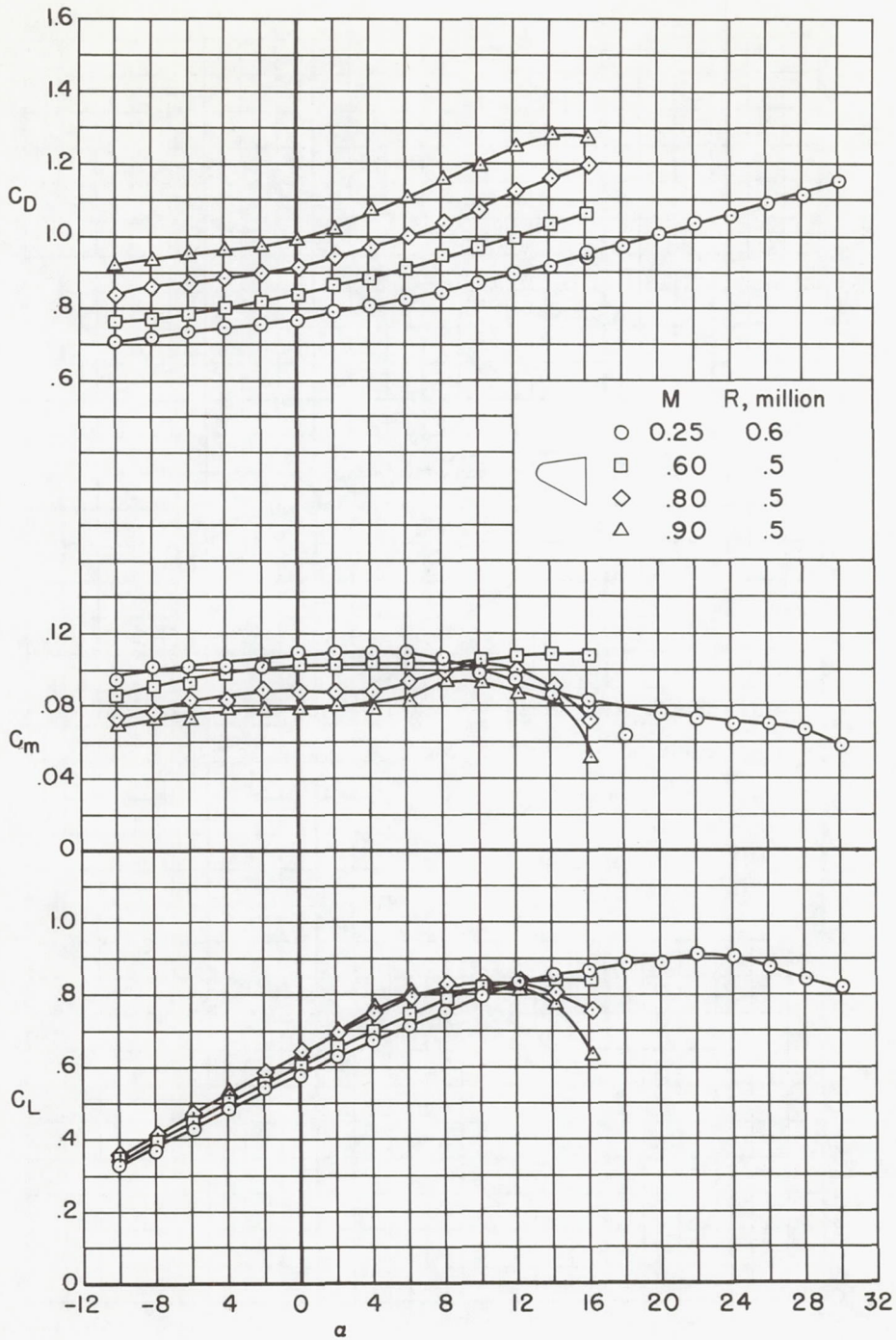


Figure 13.- The effects of Mach number on the longitudinal aerodynamic characteristics of the body with the rounded top edge.

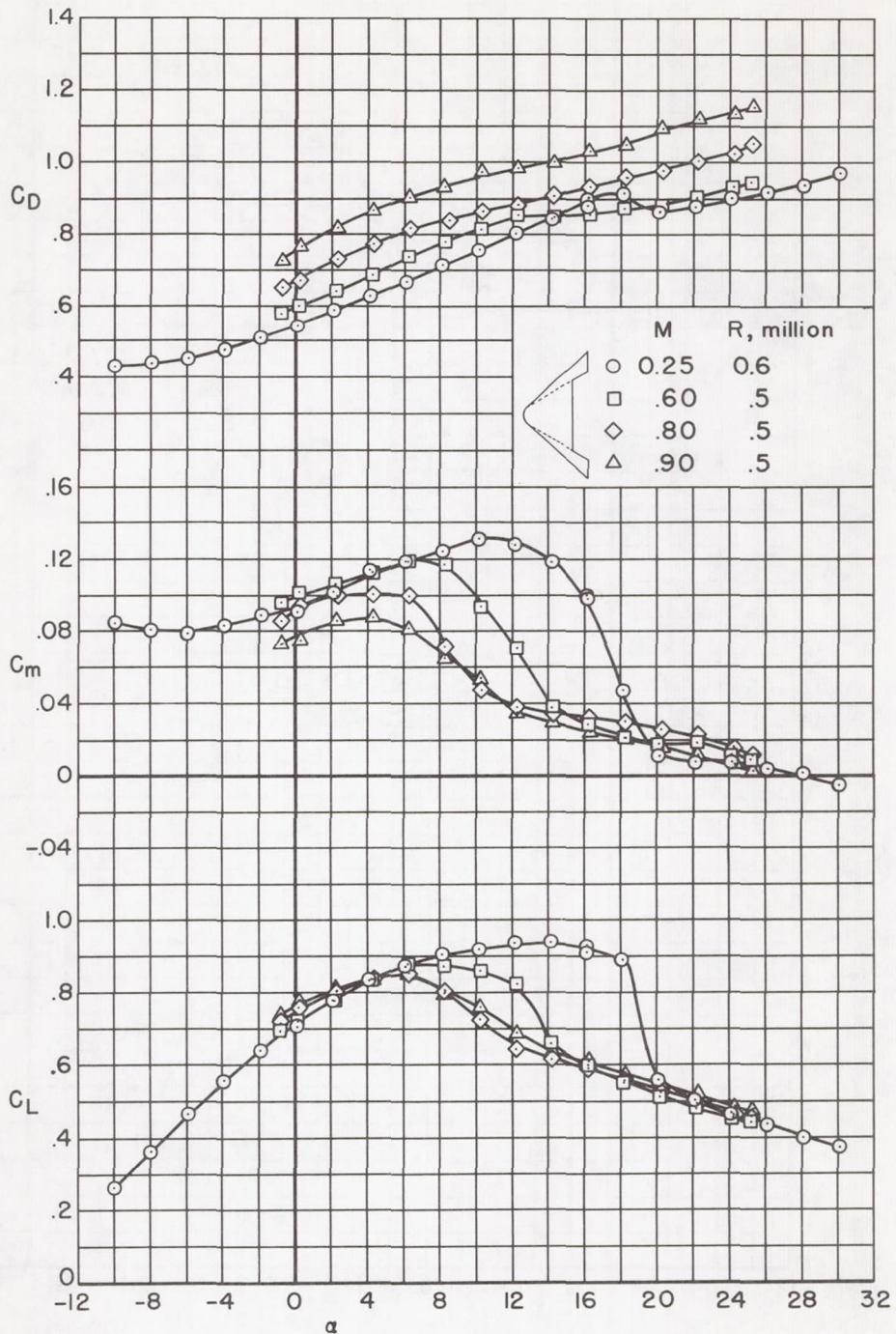


Figure 14.- The effects of Mach number on the longitudinal aerodynamic characteristics of the model with the basic body and the 47.6° sweptback wing.

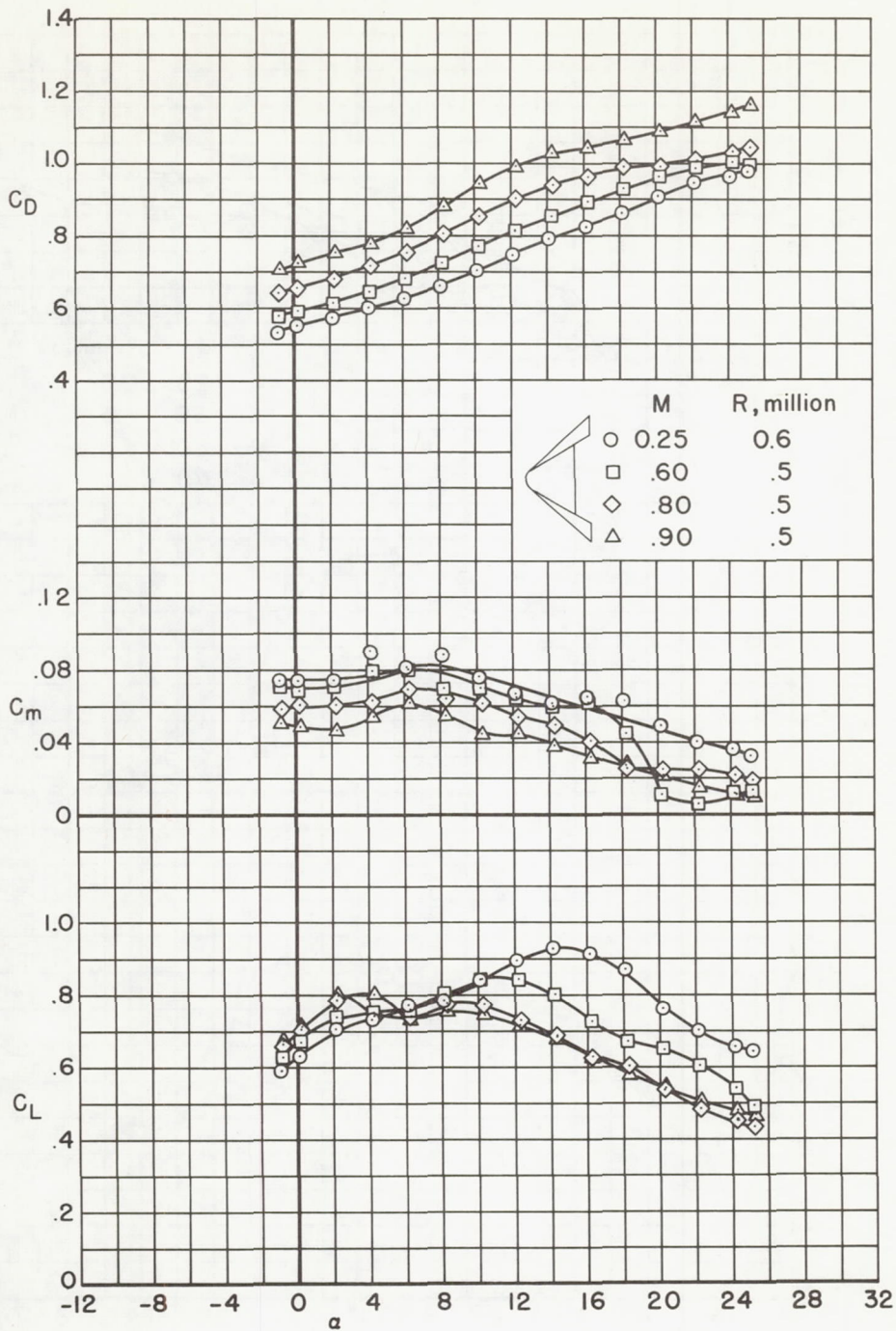


Figure 15.- The effects of Mach number on the longitudinal aerodynamic characteristics of the model with the body having the rounded top edge and the 47.6° sweptback wing.

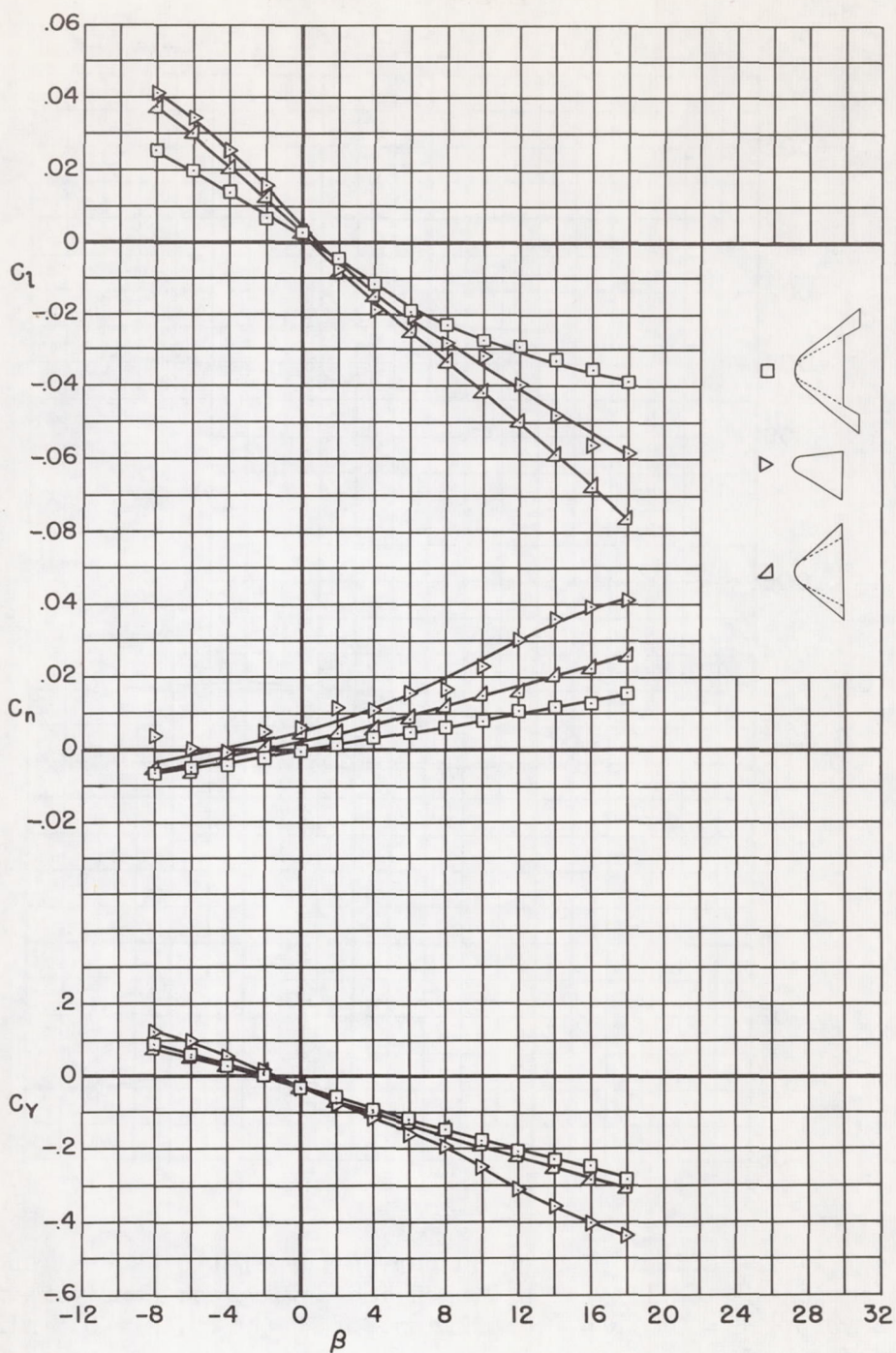


Figure 16.- Lateral and directional aerodynamic characteristics of a wingless and two winged configurations; $M = 0.25$, $R = 0.6$ million, $\alpha \approx 10.5^\circ$.

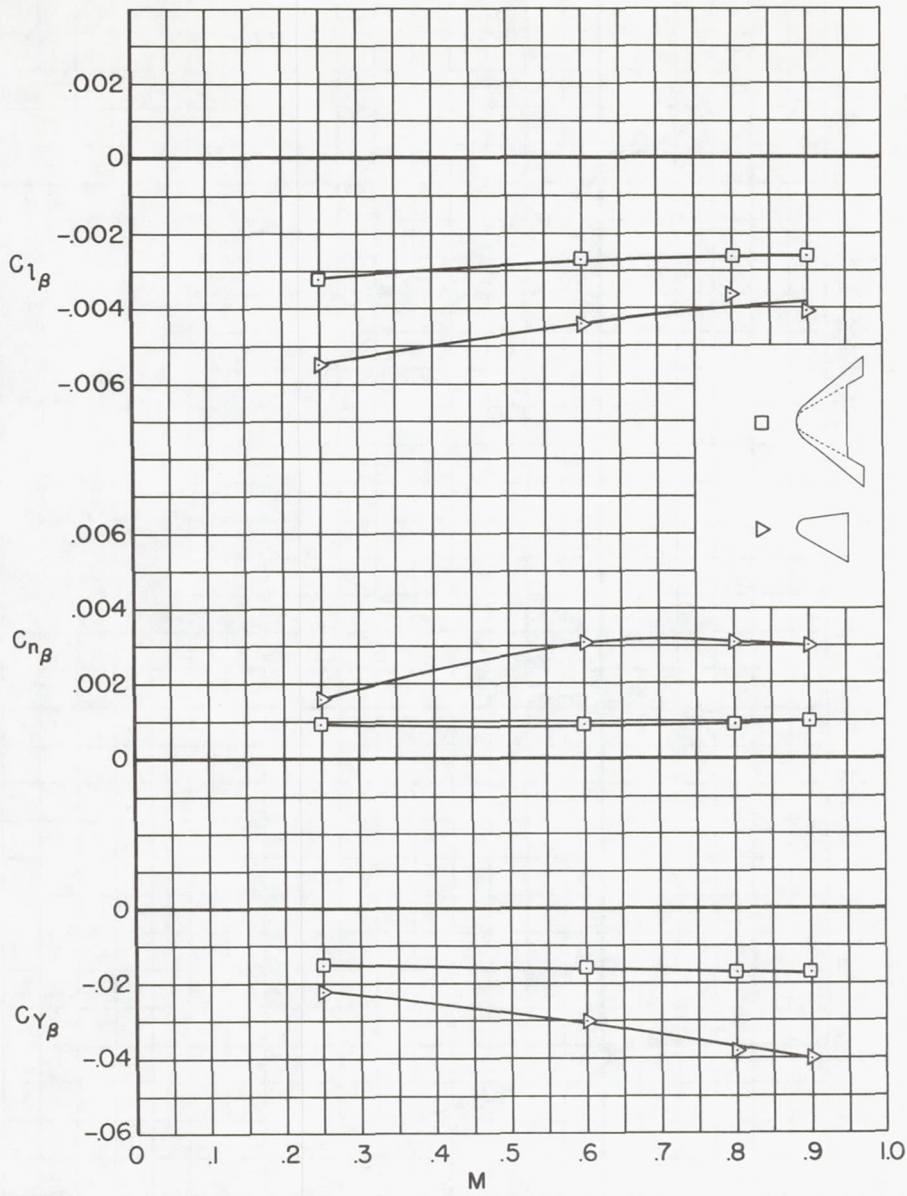


Figure 17.- The effect of Mach number on the static lateral and directional stability of a winged and a wingless configuration; $\alpha \approx 10.5^\circ$, $\beta = 0^\circ$, $R = 0.6$ million for $M = 0.25$, $R = 0.5$ million for $M \geq 0.60$.

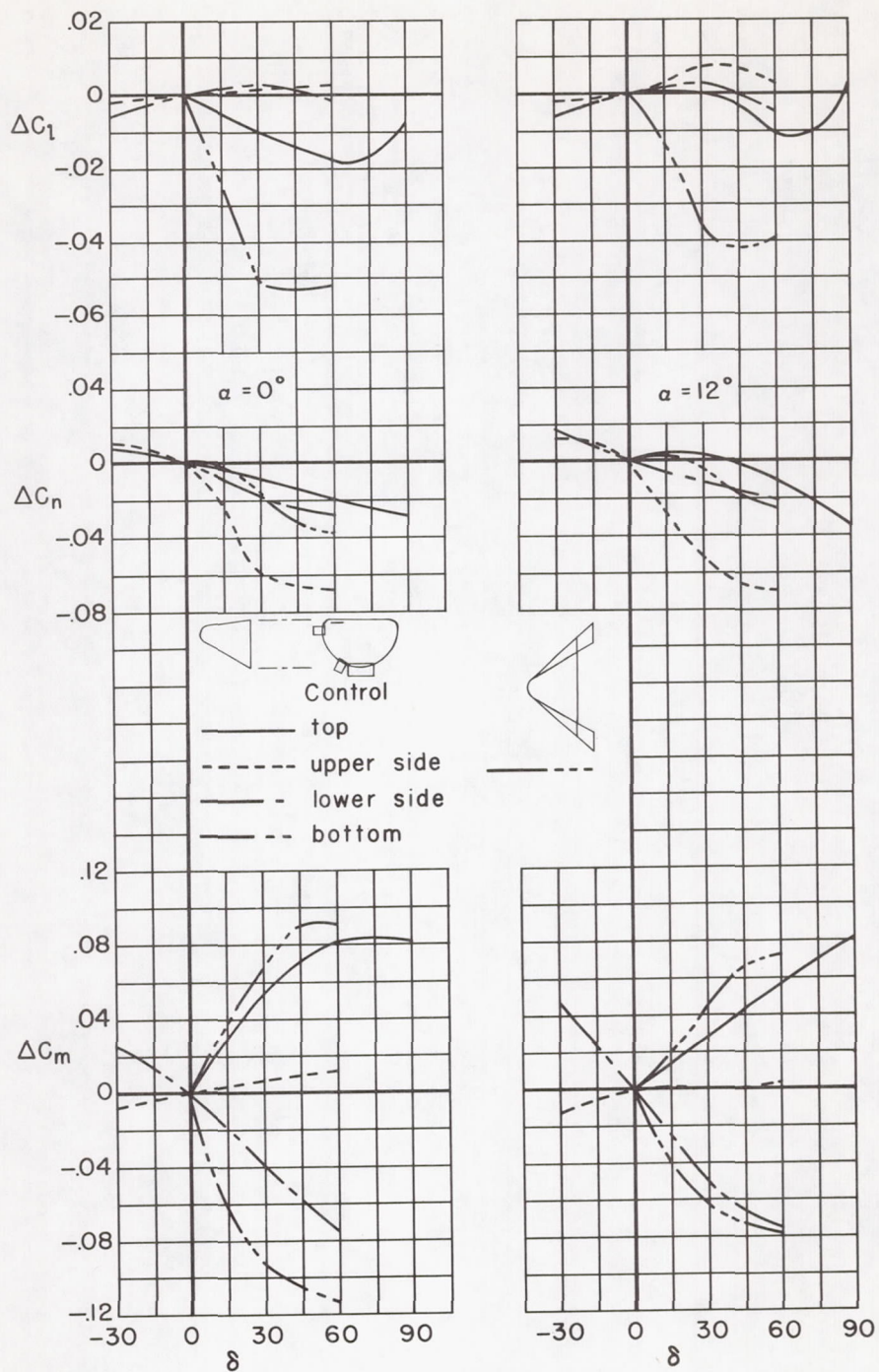


Figure 18.- Control effectiveness; $M = 0.25$, $R = 0.6$ million, $\beta = 0^\circ$.